

MODELING ON A BLUNT PROJECTILE WITH A NOSE-CABIN-COLUMN PERFORATING INTO METALLIC PLATES

X.W. Chen¹⁺, Y.H. Hang², Y.B. Yang¹ and Z.H. Lu¹

¹ Institute of Structural Mechanics, China Academy of Engineering Physics,
P.O. Box 919-414, Mianyang City, Sichuan Province, 621900, China

² Institute of Applied Physics and Computational Mathematics, P.O.Box 8009, Beijing, 100088
⁺corresponding author. E-mail: chenxiaoweintu@yahoo.com

A lower density nose-cabin-column (NCC), i.e., an assembly of seeker and guidance/control unit, is installed in front of warhead for a real semi-piercing weapon. It acts as an energy buffer in the perforation of metallic plates and notably affects the terminal results of warhead. The present paper constructs a rigid-plastic model consisting of transverse shear, bending and membrane deformations to assess the effect of NCC on the perforation of metallic plates by a stubby warhead. Especially the effect of ahead structural response, induced by NCC impacting target, is considered in the analysis. Analytical formulae for the ballistic performance are obtained for a range of plate thickness, which agree with available experimental results on the perforation of metallic plates struck by semi-piercing warhead.

INTRODUCTION

We call an assembly of seeker and guidance/control unit as a nose-cabin-column (shorten as NCC in the manuscript), which is always installed in the front of a warhead for a semi-piercing weapon [seeing Fig.1]. Comparatively, Kim, et al.[1] called it as the front section of warhead. Usually NCC has low density and honeycomb compositions, and it damages and crashes easily rather than the warhead projectile.

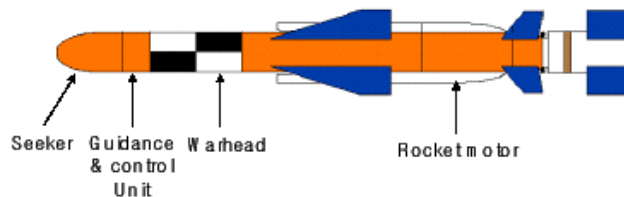


Figure 1. Generic missile structure [1]

The influence of NCC on perforation has been confirmed positive for the integrity of warhead structure. The ahead structural response of target initiated by NCC impact is beneficial to decrease the relative velocity between projectile and target and to increase the time duration of perforation. The accumulation of crashed NCC on the tip of projectile acts as a buffer to relax the impact loading. Essentially the effect of NCC should be involved in the terminal effect of semi-piercing warhead striking targets.

Both local impact effect and global structural response may be involved in the perforation of metallic plates[2,3]. However, all the existing models are unable to predict the effect of NCC on the perforation of metallic plates. The present paper further develop Chen and Li[3] to account for the effect of NCC on the perforation [4].

AHEAD STRUCTURAL RESPONSE OF TARGET INITIATED BY NCC

Considering a semi-piercing warhead of diameter d normal impacts a thin metallic plate at initial velocity V_i (Fig.2a). The thickness and density of target are H and ρ , respectively. The length and density of NCC are l and ρ_1 , respectively. It is assumed that a part of NCC of mass m crashes and splashes, and initiates a velocity field of target plate, as shown in Fig. 2b, while a total mass M of projectile and the attached accumulation of NCC still perforate the thin metallic plate at initial velocity V_i . Therein the total mass of projectile and NCC is $(M+m)$.

The initiated velocity field of target plate induced by the impact of NCC is

$$\dot{W} = \begin{cases} V_0 & 0 \leq r \leq d/2 \\ 2V_0(\xi - r)/(2\xi - d) & d/2 < r \leq \xi \\ 0 & \xi < r \leq D/2 \end{cases} \quad (1)$$

where $r = \xi$ represents the final location of bending hinge.

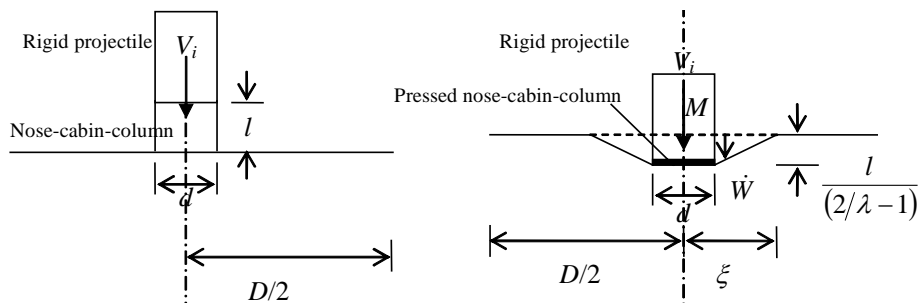


Figure 2. Schematic of a semi-piercing warhead impacting a target plate

At $r = \xi$, according to Chen and Li[3], the bending moments in radial and hoop directions of a rigid, perfectly plastic circular plate, are $M_r = -M_0$ and $M_\theta = M_0$, respectively. $M_0 = \sigma_y H^2 / 4$ and σ_y are the fully plastic bending moment and yielding strength, respectively. The shear resistance per unit length of the plate at position $r = \xi$ is $Q = [\partial(rM_r) / \partial r - M_\theta] / r = -2M_0 / \xi$, which, together with the momentum conservation in the impact direction,

$$-2\pi \int_0^{t_-} \xi Q dt = 4\pi M_0 t_- = mV_i - 2\pi\rho H \int_0^\xi \dot{W} r dr \tag{2}$$

occurs at $t_0 = 0$ when NCC completes its strike and projectile reaches plate, and the duration of NCC impacting target is t_- . Simplify, assuming the velocity field of target plate (\dot{W} or V_0) increases linearly. At time $t_0 = 0$ there exists a geometric relationship,

$$l = \left(V_i - \frac{V_0}{2} \right) t_- \tag{3}$$

with combining Eqs.(2) and (3), we have

$$\frac{\beta}{2} V_0^2 - (1 + \beta) V_i V_0 + 2 \left(V_i^2 - \frac{4\pi M_0 l}{m} \right) = 0 \tag{4}$$

in which, the dimensionless numbers β and η_1 are, respectively,

$$\beta = 2\eta_1 \left[4(\xi/d)^2 + 2\xi/d + 1 \right] / 3 \tag{5}$$

$$\eta_1 = \frac{\rho\pi d^2 H}{4m} = \frac{\rho H}{\delta\rho_1 l} \tag{6}$$

$\delta = \frac{4m}{\rho_1\pi d^2 l}$ is mass ratio of transverse dispersal of NCC. It leads to

$$V_0 = \lambda V_i \tag{7}$$

$$t_- = 2l / [(2 - \lambda) V_i] \tag{8}$$

The impact of NCC also may not induce an ahead structural response if the target plate is thick enough, i.e., $V_0 = 0$. Eq.(2) requires, $4\pi M_0 t_- \geq mV_i$, and it leads to

$$\chi \geq \frac{1}{2} \sqrt{\delta \Phi_J \frac{\rho_1}{\rho}} \quad (9)$$

in which $\chi = H/d$ is the dimensionless plate thickness, and $\Phi_J = \rho V_i^2 / \sigma_y$ is Johnson damage number. In other word, a metal plate becomes so strong that may be regarded as rigid when a soft NCC striking it. Finally, we have

$$\lambda = \begin{cases} \left[(1 + \beta) - \sqrt{(1 - \beta)^2 + \frac{16\beta\chi^2}{\delta\Phi_J} \cdot \frac{\rho}{\rho_1}} \right] / \beta, & \chi < \frac{1}{2} \sqrt{\delta\Phi_J \frac{\rho_1}{\rho}} \\ 0, & \chi \geq \frac{1}{2} \sqrt{\delta\Phi_J \frac{\rho_1}{\rho}} \text{ or } l = 0 (\text{without nose-column}) \end{cases} \quad (10)$$

At time $t_0 = 0$ when NCC ceasing strike, the corresponding deformation of target plate and the displacement of projectile are further formulated as

$$W_1 = l / (2/\lambda - 1) \quad (11a)$$

$$W_0 = l / (1 - \lambda/2) \quad (11b)$$

With including the effects of NCC, a similar formulation to Chen and Li[3] may be conducted with modified initial conditions. More details can be found in [4]. The scenarios of medium plate and thin plate are studied in next two sections, respectively.

PERFORATION OF MEDIUM PLATES, $\chi_1 < \chi \leq \sqrt{3}(A + B\Phi_J)/4$

For a relatively thick target, only shear and bending responses are considered. In this scenario, usually we have $\chi_1 \approx 0.1 \sim 0.2$, and A and B are dimensionless material constants used in the dynamic cavity expansion theory. The initial conditions, i.e., the initial velocity of target plate, is $\dot{W}_1 = V_0$ and $W_1 = l / (2/\lambda - 1)$ at time $t_0 = 0$. Following the same procedure in Chen and Li [3], the ballistic limit can be evaluated as

$$V_{BL} = \frac{2}{(1 - \lambda)} \sqrt{\frac{2k\chi(1 + \eta)(\eta + \vartheta)}{\sqrt{3}}} \cdot \sqrt{\frac{\sigma_y}{\rho}} \quad (11)$$

where $\eta = \rho \pi d^2 H / 4M$. Similarly, a velocity jump exists at the ballistic limit,

$$V_{Jump} = \dot{W}_0(t_{BL}) = \frac{[\mathcal{G}(1 + \lambda\eta) + \lambda\eta(1 + \eta)]}{(1 + \eta)(\eta + \mathcal{G})} V_{BL} > 0 \tag{12}$$

If $V_i \geq V_{BL}$, the residual velocity can be formulated as

$$V_r = \frac{[\mathcal{G}(1 + \lambda\eta) + \lambda\eta(1 + \eta)]V_i + \eta(1 - \lambda)\sqrt{V_i^2 - V_{BL}^2}}{(1 + \eta)(\eta + \mathcal{G})} \geq V_{Jump} \tag{13}$$

\mathcal{G} is a dimensionless constant determined by $\chi = H/d$ and the location of the bending hinge ξ , as defined in Chen and Li[3].

There is $\lambda = 0$ if either no NCC ($l=0$) exists before the warhead or the target plate is thick enough ($\chi \geq \sqrt{\delta\Phi_J \rho_1/\rho}/2$), and the present model degenerates into [3]. If $\mathcal{G} = 0$ and $\lambda = 0$ are simultaneously satisfied, it further degenerates to [2].

PERFORATION OF THIN PLATE, $\chi < \chi_1$

The corresponding initial condition is modified as $\dot{W}_1 = V_0 = \lambda V_i$ and $W_1 = l/(2/\lambda - 1)$ at time $t_0 = 0$. Following the same procedure in [3], we have

$$\frac{f}{g} t_{BL} \sin(gt_{BL}) + \frac{2\eta\sigma_y}{\sqrt{3}(1 + \eta)\rho d} t_{BL}^2 - \frac{f}{g^2} [1 - \cos(gt_{BL})] = kH \tag{14a}$$

$$V_{BL} = \frac{1}{(1 - \lambda)} \left[\frac{f}{g} \sin(gt_{BL})(1 + \eta) + \frac{4\eta\sigma_y}{\sqrt{3}\rho d} t_{BL} \right] \tag{14b}$$

$$V_{Jump} = \lambda V_{BL} + f \sin(gt_{BL})/g \tag{14c}$$

It shows that a velocity jump V_{Jump} at ballistic limit also exists when membrane response in a plate becomes important with the decrease of plate thickness.

If $V_i \geq V_{BL}$, the projectile perforates the plate and its residual velocity is

$$V_r = \frac{1}{(1 + \eta)} \left[(1 + \lambda\eta)V_i - \frac{4\eta\sigma_y}{\sqrt{3}\rho d} t_{1*} \right] \tag{15a}$$

where, t_{1*} is determined by

$$\frac{1}{(1+\eta)} \left[(1-\lambda)V_i t_{1*} - \frac{2\eta\sigma_y}{\sqrt{3}\rho d} t_{1*}^2 \right] - \frac{f}{g^2} [1 - \cos(gt_{1*})] = kH, \quad t_{1*} \leq t_{BL} \quad (15b)$$

Similarly, Eqs.(14-15) should be associated with Eq.(10) to solve ballistic limit V_{BL} and velocity jump V_{Jump} as well as residual velocity V_r since λ of Eqs.(14-15) depends on initial velocity V_i (or ballistic limit V_{BL}).

It should be noted that this analysis applies only for the plug-induced perforation of thin plates. The present model reduces to Chen and Li[3] if $\lambda=0$, i.e., no nose-cabin-column ($l=0$) exists before the warhead.

EXPERIMENTAL ANALYSES

Five sets of complete test data in China Academy of Engineering Physics are employed for the present analysis, which are identified into three scenarios with regarding to different NCCs and target plates, as shown in Table 1. The tension strength of 902 and 921 steel are $\sigma_b = 600$ MPa and $\sigma_b = 1000$ MPa, respectively.

Figs. 3-5 show the ballistic performances of three scenarios of perforations predicted by the models. Analyses of both medium-plate and thin-plate by either present model or Chen and Li[3] approach a close prediction and agree well with the test at higher striking velocities than ballistic limit. Abbreviations of MP and TP represent medium-plate and thin-plate, respectively. However, there may be an obvious difference between theoretical predictions and test results nearby the ballistic limit. For a supersonic impact, a projectile perforates a target plate with reserving most of the kinetic energy. With further increasing the impact velocity, residual velocity of projectile will be rather close to the impact velocity which being as an asymptote.

It is concluded by the models that velocity jump occurs at ballistic limit because

Table 1. Test parameters of reduced-scale semi-piercing warheads and target plates

Test No.	Diameter of projectile(mm)	Mass of projectile(kg)	Mass of NCC(kg)	Length of NCC (mm)	Target material	Thickness of target (mm)	Diameter of target (mm)	V_i (m/s)	V_r (m/s) -test
II-05-02	155	18	3	120	902	15	780	680	634
II-05-02K	155	18	3	120	902	15	780	691	627
II-08G2K-03	155	20.8	2.3	85	921	13.5	780	678	628
V-05-1	80	2.13	0.41	61.5	902	8	400	667	615
V-05-2	80	2.14	0.41	61.5	902	8	400	201	118

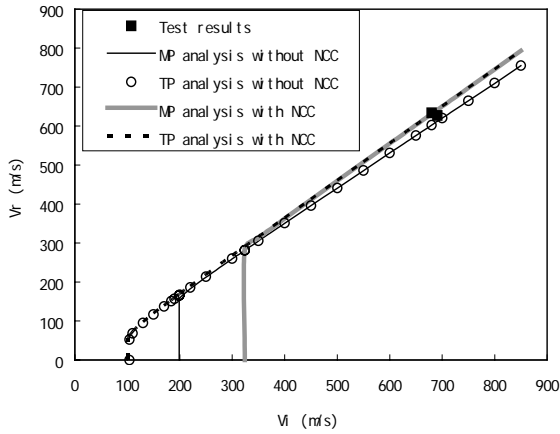


Figure 3. Test and analyses of II-05-02 & II-05-02K

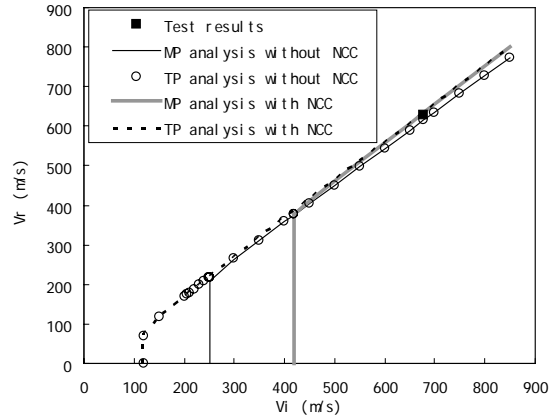


Figure 4. Test and analyses of II-08G2K-03

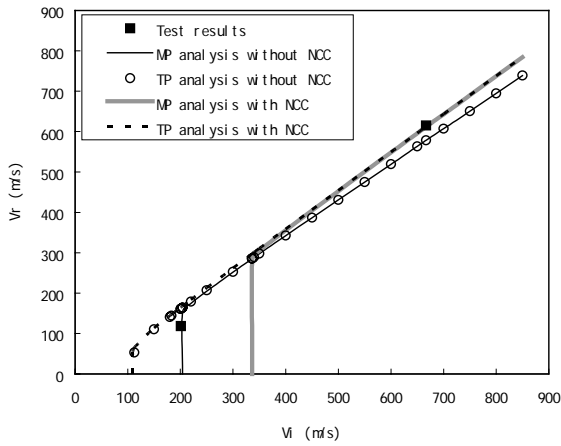


Figure 5. Test and analyses of V-05-1 & V-05-2

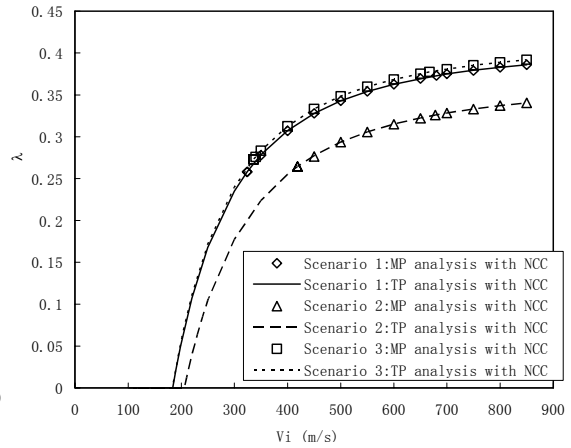


Figure 6. Relationship between $\lambda = V_r/V_i$ & V_i

of the structural response of steel plate. Similar to [3], analyses of medium-plate which involve bending effect predict higher ballistic limits and velocity jumps than the analyses of thin-plate with membrane effect. Especially, the model of projectile with NCC perforating medium-plate achieves a largest ballistic limit and a largest velocity jump. For the thin-plate analyses, either with NCC or not, their predictions of ballistic limits and velocity jumps are quite close to each other, respectively.

Both analyses of medium-plate of present model and [3] predict that V-05-2 is unable to perforate plate at initial velocity $V_0=201\text{m/s}$. Comparably, both analyses of thin-plate of present model and [3] report very close residual velocities. Normally, all

the target plates are quite thinner, i.e., $\chi = H/d \leq 0.10$, and membrane stretching of plate is more notable than its bending deformation. Combined with the prediction of supersonic perforation ($\sim 2\text{Ma}$), it is concluded that thin-plate analysis of the present model is more appropriate for the relevant experiments.

Fig. 6 shows the relationship between $\lambda = V_0/V_i$ and V_i for three scenarios of test results, where V_0 represents the initial velocity of target plate induced from ahead structural response. It demonstrates that the maximum velocity of ahead structural response of target plate induced from NCC striking, may reach 1/3 of the initial impact velocity of semi-piercing warhead. Essentially it decreases the relative velocity between projectile and target plate, and certainly decreases the impacting loading whilst increases the duration of perforation. Thus NCC is positive for a semi-piercing warhead to perforate metallic plate safely. As denoted in Fig. 6, λ decreases with decreasing V_i , and vice versa. Especially if $V_i < 200\text{m/s}$, the impact of NCC can't initiate an ahead structural response of target plate. The compositions of NCC are much softer and lighter than the metallic plate. Under subsonic impact, it is highly possible that no enough momentum transfer to the target plate. In that case, the effect of NCC on the structural response of plate is small and may be ignored. It completely agrees with the experimental observations. It is reminded that more attention should be paid for the subsonic semi-piercing warhead.

CONCLUSIONS

In the present paper, Chen and Li's model [3] is further developed to study the perforation of metallic plate struck by a blunt rigid projectile with NCC. The ahead structural response of target plate induced by the impact of NCC is further involved in the rigid-plastic analysis. More common and simple analytical formulae for the perforation performance are obtained for a range of plate thickness, which agree well with available experimental results on the perforation of metallic plates.

REFERENCES

- [1] Kim, H.S., Yeom, K.S., Kim, S.S. and Sotsky, L. Numerical simulation for the front section effect of missile warhead on the target perforation, *22nd Int. Symp. Ballistics*, 1094-1101(2005)
- [2] Recht, R.F. and Ipson, T.W. Ballistic perforation dynamics, *J. Appl. Mech.*, **30**:385-91(1963)
- [3] Chen, X.W. and Li Q.M. Shear plugging and perforation of ductile circular plates struck by a blunt projectile, *Int. J. Impact Engng.*, **28**(5):513-536(2003)
- [4] Chen, X.W., Yang, Y.B., Lu, Z.H. and Chen, Y.Z. Perforation of Metallic Plates Struck by a Blunt Projectile with a Nose-cabin-column, *Int. J. Impact Engng.*, in review, 2006